



Petters, S. S., Hilditch, T. G., Tomaz, S., Miles, R. E. H., Reid, J. P., & Turpin, B. J. (2020). Volatility Change During Droplet Evaporation of Pyruvic Acid. *ACS Earth and Space Chemistry*, 4, 741-749. [5].
<https://doi.org/10.1021/acsearthspacechem.0c00044>

Peer reviewed version

Link to published version (if available):
[10.1021/acsearthspacechem.0c00044](https://doi.org/10.1021/acsearthspacechem.0c00044)

[Link to publication record in Explore Bristol Research](#)
PDF-document

This is the author accepted manuscript (AAM). The final published version (version of record) is available online via American Chemical Society at <https://pubs.acs.org/doi/abs/10.1021/acsearthspacechem.0c00044> . Please refer to any applicable terms of use of the publisher.

University of Bristol - Explore Bristol Research

General rights

This document is made available in accordance with publisher policies. Please cite only the published version using the reference above. Full terms of use are available:
<http://www.bristol.ac.uk/red/research-policy/pure/user-guides/ebr-terms/>

This document is confidential and is proprietary to the American Chemical Society and its authors. Do not copy or disclose without written permission. If you have received this item in error, notify the sender and delete all copies.

Volatility Change During Droplet Evaporation of Pyruvic Acid

Journal:	<i>ACS Earth and Space Chemistry</i>
Manuscript ID	Draft
Manuscript Type:	Article
Date Submitted by the Author:	n/a
Complete List of Authors:	Petters, Sarah; University of North Carolina at Chapel Hill, Environmental Sciences and Engineering Hilditch, Thomas; University of Bristol, School of Chemistry Tomaz, Sophie; IRCELYON Miles, Rachael; University of Bristol, School of Chemistry Reid, Jonathan; University of Bristol, School of Chemistry Turpin, Barbara; University of North Carolina at Chapel Hill Gillings School of Global Public Health, Department of Environmental Science and Engineering;

SCHOLARONE™
Manuscripts

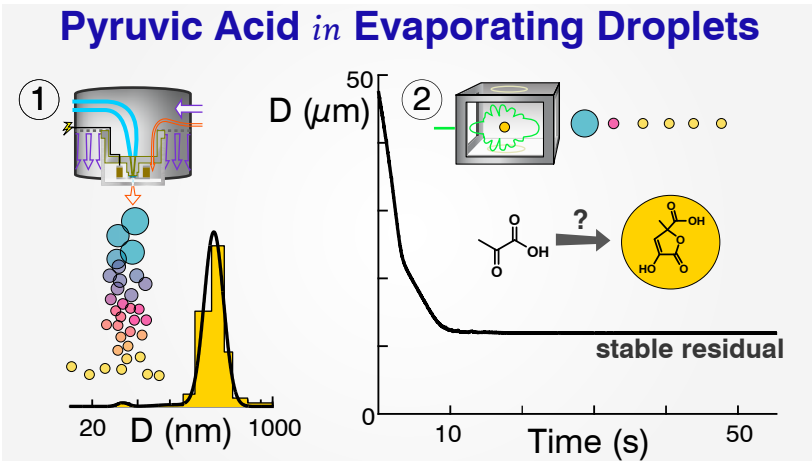
Volatility Change During Droplet Evaporation of Pyruvic Acid

Sarah S. Petters,^{1*} Thomas G. Hilditch,² Sophie Tomaz,^{1,†} Rachael E. H. Miles,² Jonathan P. Reid,² and Barbara J. Turpin¹

¹Department of Environmental Sciences and Engineering, Gillings School of Global Public Health, University of North Carolina at Chapel Hill, Chapel Hill, North Carolina, USA

²School of Chemistry, University of Bristol, Bristol BS8 1TS, UK

Manuscript for submission to ACS Earth and Space Chemistry. Feb. 11, 2020.



TOC art

Abstract

Atmospheric water-soluble organic gases such as pyruvic acid are produced in large quantities by photochemical oxidation of biogenic and anthropogenic emissions and undergo water-mediated reactions in aerosols and hydrometeors. These reactions can contribute to aerosol mass by forming less volatile compounds. While progress is being made in understanding the relevant aqueous chemistry, little is known about the chemistry that takes place during droplet evaporation. Here we examine the evaporation of aqueous pyruvic acid droplets using both the Vibrating Orifice Aerosol Generator (VOAG) and an electrodynamic balance (EDB). In some cases pyruvic acid was first oxidized by OH radicals. The evaporation behavior of oxidized mixtures was consistent with expectations based on known volatilities of reaction products. However, independent VOAG and EDB evaporation experiments conducted without oxidation also resulted in stable residual particles; the estimated volume yield was 10–30% of the initial pyruvic acid. Yields varied with temperature and pyruvic acid concentration across cloud, fog, and aerosol-relevant concentrations. The formation of low volatility products, likely cyclic dimers, suggests that pyruvic acid accretion reactions occurring during droplet evaporation could contribute to the gas-to-particle conversion of carbonyls in the atmosphere.

1. Introduction

Aerosols affect global climate and impact air quality, human health, and visibility. A substantial fraction of aerosol mass is organic, much of which is formed in-situ in the atmosphere. Despite its ubiquity, predictions of secondary organic aerosol (SOA) formation rely on incomplete mechanisms unlikely to capture aerosol production over a wide range of precursors and conditions.^{1–3} Water-mediated reactions, occurring in humidified aerosols, fogs, and cloud droplets, play an important role in converting water-soluble organic gases (WSOGs) to SOA

mass.^{4–6} However, the contribution of aqueous reactions to SOA mass remains uncertain due in part to a limited understanding of precursors and limited laboratory results to parameterize models.^{1,7–11} Quantifying the impacts of aqueous and multiphase chemistry on aerosol mass remains challenging, and a more detailed understanding of product volatility is needed.

A significant fraction of low molecular weight acids, aldehydes and carbonyls dissolve into cloud or fog droplets. In the absence of additional reactions, these WSOGs largely evaporate during water evaporation; the trace amounts that remain in the aerosol phase are determined by their partial pressure in the gas phase and activity in the aerosol matrix. However, multiphase reactions can generate low-volatility products that are retained in the equilibrated aerosol. Several important criteria determine whether aqueous processing can appreciably increase SOA mass: (1) the precursor must be abundant, (2) it must have a high vapor pressure before aqueous reactions, (3) it must have a high Henry's law coefficient and thus strongly partition into water, and (4) it must react in the aqueous phase to form less volatile products.

To date many cloud- and fog-relevant studies have focused on the aqueous OH oxidation of a limited number of compounds meeting the above criteria, such as glyoxal,^{12–14} glycolaldehyde,^{15,16} methacrolein,¹⁷ acetic acid,¹⁸ methylglyoxal,^{19–21} methyl vinyl ketone,²² phenolic compounds,²³ and pyruvic acid,^{24,25} as well as studies focusing on oxidation by singlet molecular oxygen²³ and triplet excited states of oxygen,^{23,26} photosensitization,²⁷ and photoinitiation.²⁸ The volatility of the products, or the extent to which products remain in the particle phase after water evaporation, has been determined for some of these systems but not for pyruvic acid. Studies have also shown that non-radical reactions can yield low-volatility compounds in deliquescent aerosols,^{29–32} especially for glyoxal, methylglyoxal, and isoprene-derived epoxydiols.^{29–32} Because these systems rely on catalysis, formation of oligomers is sometimes reversible; irreversible formation of low-volatility

products are generally associated with radical^{4,33,34} or ring-opening³¹ reactions due to their higher activation energy. Nevertheless, glyoxal and methylglyoxal form stable products in evaporating solutions with or without inorganic catalysts^{30,32,35} due to the reactive dicarbonyl group.³⁵ These and other accretion reactions occurring in the absence of photooxidation have been recognized as an important contributor to organic aerosol.³⁶ Evaporation of droplets concentrates solutes, shifts the solution pH, and can allow enhanced surface partitioning of surface-active compounds over short timescales, enhancing reaction rates.^{32,37–41} The droplet air-liquid interface may also accelerate reactions by confining molecules to specific orientations, enhancing their reactivity or acidity,^{42–46} and molecular partitioning to the air-liquid interface and self-organization in the surface layer can affect gas uptake and reaction rates.^{47,48}

Pyruvic acid is abundant in aerosols, fogs, and clouds, and is produced^{19,24,25,49,50} photochemically in the atmosphere^{50,51} mainly through gas-phase oxidation of aromatic hydrocarbons,^{52–54} biomass burning,⁵⁵ and aqueous OH oxidation of methylglyoxal.^{49,56} Pyruvic acid has an intermediate volatility³⁴ and partitions between the gas and aerosol phases.^{51,53,57} Studies of aqueous pyruvic acid processing have focused on photolysis^{26,56,58} and OH-radical initiated photooxidation.^{24,25,59} Evidence for dark pyruvic acid accretion reactions from environmental chamber studies shows that partitioning of pyruvic acid and other acids or carbonyls to SOA exceeds expectations based on their high vapor pressures.^{52,60} Here we extend these studies to include dark processing of pyruvic acid in evaporating cloud droplets.

In this work we examine an aspect of cloud/fog processing – the evolving volatility distribution of aqueous pyruvic acid with droplet evaporation. We also investigate changes in volatility after OH oxidation of the aqueous pyruvic acid solutions.

2. Method

Pyruvic acid evaporation experiments followed two methods and spanned concentration ranges from 10 μM to 2 M. Vibrating Orifice Aerosol Generator (VOAG)⁶¹ Evaporation and Residual Analysis (VERA) was performed for a series of solutions between 10 μM (cloud relevant) and 20 mM, a concentration range that reflects cloud concentrations and concentrations as cloud droplets evaporate. Additional pyruvic acid evaporation experiments were performed using an electrodynamic balance (EDB) at 2 M. The EDB concentration is relevant to deliquescent aerosols rather than clouds; the choice of concentrations for EDB experiments was dictated by instrumental constraints. For comparison, VERA experiments were also performed for other organic acids (10 μM –20 mM) and for aqueous pyruvic acid after OH-radical oxidation (300 μM pyruvic acid; fog-relevant concentration). An evaporation model was used to aid in the interpretation of data. VERA and EDB techniques, oxidation experiments, and modeling are described in the following paragraphs.

2.1 VOAG Evaporation and Residual Analysis (VERA)

Droplet evaporation experiments were performed for aqueous solutions of pyruvic acid (with and without OH oxidation) or other organic acids/carbonyls using VERA as described previously.¹⁶ VERA emulates cloud droplet evaporation by generating micron-scale droplets with very narrow size distributions (monodispersed and near cloud-relevant sizes),⁶² and evaporating them in a turbulent flow tube. Briefly, a VOAG (TSI 3450) was used to generate monodisperse droplets. Water evaporated rapidly and size distributions of the organic residuals were detected in real time downstream by an aerosol spectrometer (GRIMM Aerosol Technik Ainring GmbH; model 1.109). Evaporation of the organic served as a metric of its vapor pressure. Modifications to the instrument liquid feed, orifice, and flow tube following Barr et al.^{63–65} are described in the

Supporting Information (SI) alongside the measurement schematic (Figure S1); analysis is described below. A 20 μm orifice was used and produced 35 ± 0.053 μm droplets under typical conditions. For an involatile solute, solutions of 9.4 μM to 19 mM result in dry residual diameters (hereafter referred to as “nominal diameters”) of 0.30 to 3.9 μm . Equilibrium water retention was estimated from molar volume^{66,67} and did not exceed 2–5% of nominal particle volume. Calculation details and spectrometer calibration are described in the SI. Observed residual diameters were taken as the peak of the measured size distribution. The evaporation process and the influence of physicochemical properties are described in the Evaporation Modeling section below.

2.2 Evaporation in the Electrodynamic Balance (EDB)

Pyruvic acid solutions were evaporated in an EDB as described previously.^{68–70} Aqueous solutions of 2 M pyruvic acid in ultrapure water were prepared. The higher concentration was necessary due to experimental constraints and is comparable to total organic carbon (TOC) in deliquescent aerosols.⁷¹ Droplets were produced using a piezoelectric droplet-on-demand generator and trapped in an electrodynamic potential well generated from two pairs of concentric cylindrical electrodes. Trapped droplets evaporated in a 3 cm s^{-1} N_2 gas flow at constant temperature and relative humidity (RH). A green laser (532 nm) illuminated the droplet and the scattered diffraction pattern was used to determine droplet size with a time resolution of 10 ms. Experiments were performed at 10, 20, and 25°C. Additional tests included variable RH or a different initial solvent. EDB experiments were conducted at the University of Bristol. Each experiment was repeated 4–9 times.

2.3 Oxidation and Product Quantification for Pyruvic Acid + OH(aq)

Aqueous solutions of 300 μM (10.8 ppm-C) pyruvic acid were oxidized via OH radicals using a water-jacketed 1 L photochemical batch reactor at 25°C as described previously and products were quantified by ion chromatography.^{19,72} The pyruvic acid concentration is similar to the total organic carbon found in fog water or polluted cloud water.^{73,74} Estimated steady-state [OH] was $\sim 5.5 \times 10^{-12}$ M during pyruvic acid oxidation.⁷⁵ Additional experimental details are provided in the SI. Typical cloudwater [OH] is believed to be 10^{-13} M or lower.^{76,77} We used higher concentrations to focus on OH initiated reactions and to access a wide range of equivalent atmospheric oxidation timescales from minutes to days.⁷⁶

Aliquots of 10–12 mL were withdrawn at increasing time intervals and offline analysis was performed within one day. Samples were analyzed for organic acids using ion chromatography (IC; Dionex ICS-3000) and for TOC (Sievers M9). Evaporation experiments using VERA were performed for a subset of aliquots directly and after serial dilution.

3. Evaporation Model

Evaporation of pyruvic acid solution droplets in VERA was estimated following Su et al.^{70,78} and Bilde et al.^{79,80} A model description is included in the SI. Particle velocity relative to the gas was assumed to be the terminal settling velocity⁸⁰ and the gas-phase concentration of organic was assumed to be zero in the flow tube (we estimate it was < 2% saturated). Pyruvic acid diffusivity in air was estimated to be $8.1 \times 10^{-2} \text{ cm}^2 \text{ s}^{-1}$ via the Hirschfelder equation.^{79,81,82} VERA was emulated by modeling water evaporation from the droplet until reaching the organic nominal residual diameter, then modeling organic evaporation until the time of observation by the spectrometer. Modeled RH was 11% and measured RH was 10–13%. In addition to modeling binary water-organic solutions, we modeled scenarios introducing a second solute with lower

vapor pressure (10^{-4} Pa) into the droplet. The modeled residual diameter is mainly controlled by aqueous solution concentration, organic vapor pressure, evaporation time and RH.

Figure S2 shows the evaporation model for the VERA technique. After water evaporation the “nominal diameter” of the residual organic particle is calculated from the initial solution concentration assuming no evaporation of the organic (x-axis). However, because the organic matter partially evaporates, the “observed diameter” (residual diameter observed by the spectrometer), on the y-axis, is dependent on the organic vapor pressure. Panel A shows the expected observation for a pyruvic acid-like compound with different assigned vapor pressures. The line spacing shows the vapor pressure resolution for organics of similar size and functionality. Vapor pressures (p^o) between 3 and 0.3 Pa are resolved under current operating conditions. Panel B shows the result of adding an involatile second solute to the modeled droplets, simulating the conversion of some of the pyruvic acid to a less volatile compound. The inset is a three-bin volatility basis set for this setup, where bin 1 ($p^o \leq 0.3$ Pa) describes compounds that do not evaporate, bin 2 ($0.3 \leq p^o \leq 3$ Pa) describes compounds that partially evaporate, and bin 3 ($p^o \geq 3$ Pa) describes compounds evaporating completely before detection.

Figure S2 shows the droplet size after 4.9 s of evaporation (the flow tube residence time), to simulate what is measured by VERA. It does not show the time-resolved evaporation of multiple solution components because VERA uses a fixed observation time and multiple experiments with different concentrations to generate a plot of nominal vs observed diameter. The model is therefore helpful in interpreting the data. The presence or absence of curvature in the observations is an indication of the volume fraction of solute in each of the volatility bins shown in Panel B. If observations include curvature, some component falls in bin 2 and its vapor pressure can be determined with greater precision. In the absence of curvature, all components are in bins 1 and 3,

with the fraction in bin 1 shown by the angle of the line of observed diameters. For example, if the angle is 0° (x-axis), all compounds are in bin 3 (evaporated), and if the angle is 45° (1:1 line), all compounds are in bin 1 (did not evaporate). Evaporation data (nominal vs observed residual diameter) falling on a line between 0° and 45° in Figure S2 panel B are fitted and the slope of the fit line is indicative of the fraction of organic that did not evaporate.

4. Results and Discussion

In the following paragraph we show that OH oxidation of pyruvic acid slowly produces acetic and oxalic acids, consistent with known mechanisms, and that oxidation reduces the volatility of the mixture. Then we present the dark evaporation of aqueous pyruvic acid using VERA and EDB techniques. Despite expectations based on the vapor pressure of pyruvic acid, droplet evaporation resulted in the formation of stable residual particles. A possible oligomerization mechanism and atmospheric implications are discussed.

4.1 Oxidation Experiments

Figure 1 shows the evolving composition of 300 μM aqueous pyruvic acid undergoing OH radical-initiated oxidation over 150 min, as determined by ion chromatography. Oxidation converts pyruvic acid mainly to oxalic and acetic acid. This delayed formation of oxalic acid is consistent with the known multistep oxidation mechanisms.^{19,75,83} Evaporation of these solutions and their volatility is discussed below.

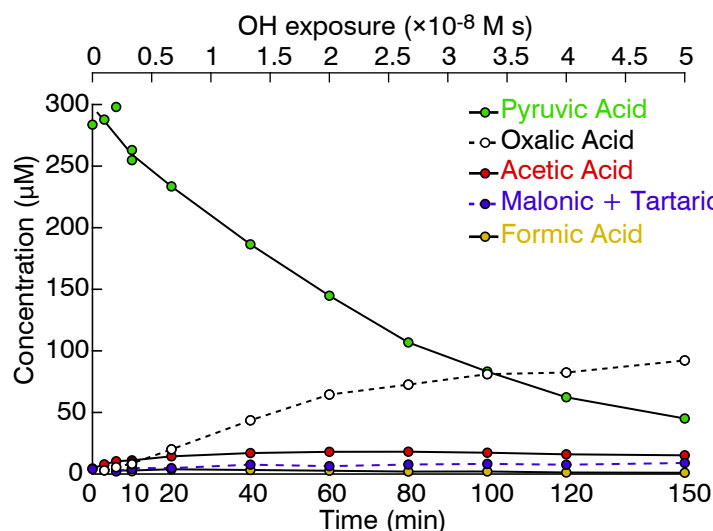


Figure 1. Oxidation products of pyruvic acid + OH(aq) as quantified by ion chromatography.

4.2 VERA Evaporation Experiments

Figure 2 shows the results of VERA experiments for oxidized pyruvic acid and for (dark) standard solutions of pyruvic acid or other organics. As oxidation converts pyruvic acid to oxalic acid, the net result is lower volatility, as seen by an increase in the slope of Figure 2A. By comparing the slope of the observations with the modeled lines we estimate that the volume fraction of organics in volatility bin 1 ($p^o < 0.3$) was ~60% after 150 min of oxidation. The remaining 40% was likely unreacted pyruvic acid and volatile products such as acetic and formic acids. Panel B shows evaporated standard solutions. Most organics longer than 3 carbons did not evaporate before observation and thus fall in bin 1 and are observed on the 1:1 line. Additional experiments falling on the 1:1 line were omitted for clarity (oxalic, tartaric, and malic acids). Compounds evaporating completely fall in bin 3 ($p^o > 3$) and are observed on the x-axis. Pyruvic acid solutions evaporated partially (dark blue). As described in section 3, the lack of curvature in the observation indicates that some of the solute was volatile (pyruvic acid falls in volatility bin 3) and some of the solute did not evaporate (unknown compound falling in volatility bin 1). Assuming

volume additivity, $\sim 10 \pm 5\%$ of the pyruvic acid by volume was converted to a lower volatility product. The volume conversion is likely lower when accounting for solvation effects.

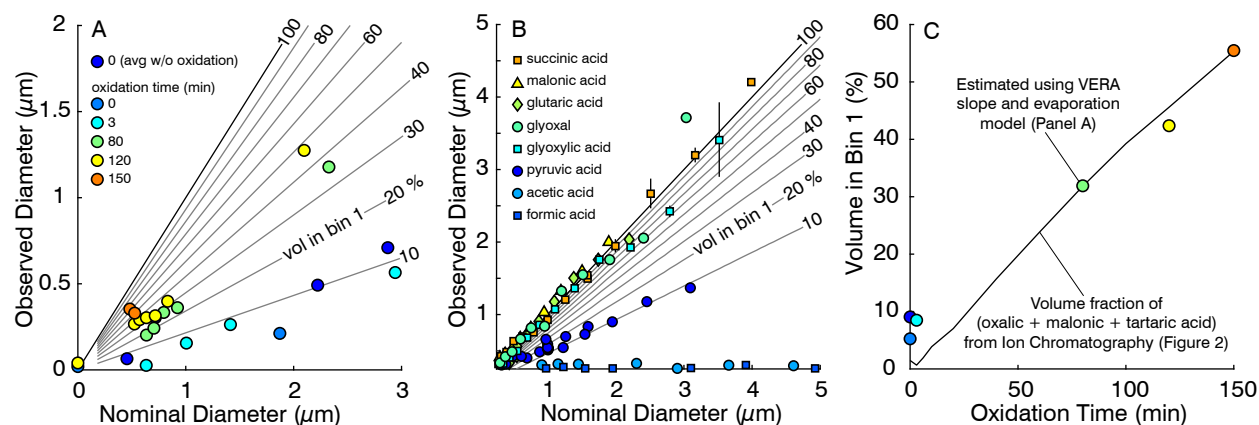


Figure 2. VERA evaporation of (A) oxidized pyruvic acid solutions (background subtracted) and (B) aqueous pyruvic acid and other compounds. Observed diameter is by spectrometer and nominal diameters are involatile-equivalent diameters from solution concentration. Grey lines show estimated fraction with lower volatility (volatility bin 1; $p^o < 0.3$ Pa). (C) Percentage of solute in bin 1 ($p^o < 0.3$) estimated independently from VERA slope (circles; data from panel A) and from IC data (line; data from Figure 1).

Figure 2C shows that oxidation shifted products into the lower-volatility bin (bin 1). Colored circles indicate the fitted slope of VERA experiments in Panel A and the black line is an independent estimate of non-evaporating compounds for the same mixtures using ion chromatography, shown in Figure 1. The close agreement between these two estimates of evaporation corroborates the VERA model. The exception is near 0 minutes of oxidation, where evaporation of the pyruvic acid produced a 10% unknown residual (see blue circles, Figure 2C). Further experiments investigating this phenomenon were performed using the EDB and are detailed below.

4.3 EDB Evaporation Experiments

Figure 3 shows the evaporation of pyruvic acid solutions in the EDB. The sequential evaporation of water, pyruvic acid, and an unknown low-volatility substance is clearly delineated by two sharp changes in evaporation rate (Panel A). Evaporation rate slowed as remaining droplet constituents became less volatile. Abruptly raising the RH did not change the final residual diameter (Panel B). In the evaporation of pyruvic acid + isopropanol (Panel C) the sequential evaporation of solvent and pyruvic acid is also observed, again resulting in a less volatile residual. The volume conversion of pyruvic acid to low-volatility residual (assuming volume additivity and constant density equal to that of pyruvic acid) was ~15–30% across all EDB experiments.

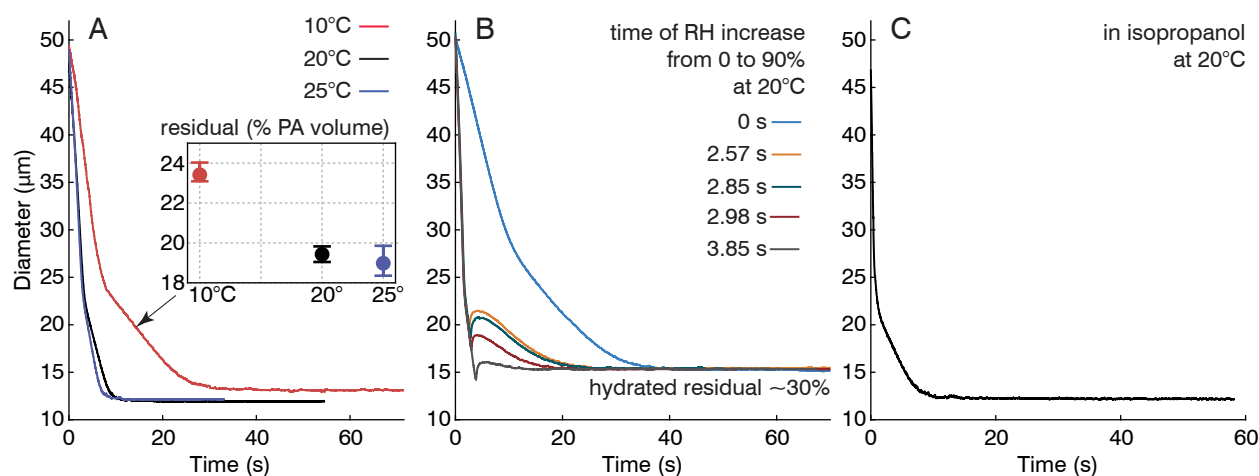


Figure 3. Evaporation of 0.1 mass fraction pyruvic acid solution droplets as observed by the EDB. (A) aqueous pyruvic acid evaporating in dry N₂ at three gas-phase temperatures. (inset) residual volumes at different temperatures. (B) aqueous pyruvic acid response to abruptly increasing RH during evaporation (at different times as indicated), (C) pyruvic acid in isopropanol evaporating at 20°C.

Varying experimental conditions affected the production of the low-volatility component. Figure 3A shows that the residual mass of low-volatility product increases at colder temperatures, demonstrating that the sustained period of high pyruvic acid concentration in the evaporating droplet has a greater effect on the reaction rate than the reduction in molecular collisions expected

at low temperatures. The volatility of the residual remained below the limit of quantification by EDB ($<5 \times 10^{-3}$ Pa) at all temperatures. Additional experiments operating on much longer timescales would have been necessary to quantify the evaporation of the formed particles. Although vapor pressure increases with increasing temperature, the effect of temperature-dependent vapor pressure on the evaporation of a single compound would result in different evaporation rates and not different yields. Comparison at different initial droplet concentrations (VERA vs EDB) shows a modest enhancement in volumetric yield at higher initial concentration. When RH was increased from 0% to 90% at different times during droplet evaporation (Figure 3B), the observed residual diameter was unchanged. Note that the residual here is larger due to equilibrium water uptake (hygroscopicity estimate of $\kappa \sim 0.015$,⁸⁴ which comparable to that of larger molecules found in SOA⁸⁵). This indicates that changing the hygroscopically-bound water in the evaporating pyruvic acid solution does not speed up the low-volatility product formation. In Panel C, evaporating the pyruvic acid in pure isopropanol resulted in evaporation rates and residuals similar to those of aqueous solutions. Because carbonyls do not undergo hydration reactions to form gem-diols as readily in isopropanol as they do in water, this suggests that the reaction producing the residual is not accelerated by the formation of a gem-diol as observed for glyoxal.³⁵

4.4 Proposed Mechanism for Self-Reaction of Pyruvic Acid

Potential formation mechanisms and structures of a low-volatility residual are now discussed. The residual volume is larger than the stated pyruvic acid impurity of 2% (all EDB experiments used brand-new stock), and several independent sources of pyruvic acid standards produced similar results. Some of this residual may form in the stock solution prior to use; however, the changing volumetric yields with changing temperatures suggests that reactions occur during

evaporation experiments. Evaporation rates of the low volatility residual were below detection, thus the influence of temperature on vapor pressure did not affect the observed yield. Gas-phase impurities are ruled out with the EDB and are unlikely with VERA.

Pyruvic acid exists as several species in solution and these equilibria are shifted by the changing pH during evaporation. The carboxylic acid group can deprotonate to form the pyruvate anion and the keto group can hydrate to form a gem-diol or tautomerize to form an enol. At room temperature, roughly 10% of pyruvate, or 60% of pyruvic acid, forms a diol.⁸⁶ Equilibrium between these forms of pyruvic acid is complicated by the high surface-to-volume ratio and rapid removal of both water and the volatile carboxylic acid form of pyruvic acid during evaporation of droplets.^{37,42,44}

The formation of C–O–C bonds by attack of an ROH group on the double bond of either the carboxyl group or the keto group of pyruvic acid is plausible. For example, acid-catalyzed esterification may convert the carboxyl group to an ester. In this reaction, the gem-diol of a hydrated pyruvic acid molecule attacks the double bond of the carboxyl group of another pyruvic acid molecule. In isopropanol, the isopropanol can attack the carboxyl double bond, producing a similar ester (Figure 3C). Either isopropanol or the pyruvic gem-diol may attack the hydrated keto group of another pyruvic acid molecule, forming a hemiacetal and potentially repeating to form an acetal, as has been reported for glyoxal.⁸⁷ An acetal may be stable against hydrolysis upon the removal of pyruvic acid and water from the droplet.

Aldol addition and condensation reactions occur by the attack of the enol tautomer of pyruvic acid on a protonated keto group of another molecule. Figure S3 shows a proposed mechanism with a cyclic dimer as a potential end product of the aqueous evaporation experiments in this work. Pyruvic acid tautomerizes readily in solution,⁸⁸ and aldol addition can proceed without hydration of the keto group to a gem-diol. Self-reactions by aldol addition have been reported for

286 methylglyoxal and glyoxal³⁰ and for pyruvic acid in both dark and photochemical reaction
287 systems.^{56,89}

288 4.5 Atmospheric Implications

289 Pyruvic acid has diverse removal processes in the atmosphere, where it can partition between
290 aerosol, aqueous, and gas phases and can dissociate, hydrate, or tautomerize in solution. The
291 primary source of pyruvic acid outside of urban areas is the aqueous phase OH oxidation of
292 isoprene oxidation products such as methylglyoxal and lactic acid,^{19,57,90} and under dry conditions
293 it is found largely in gas phase (rather than the aerosol), where it is removed by direct photolysis
294 and dry deposition.^{51,53,91} In the presence of fogs and clouds pyruvic acid can be retained by (or
295 re-partition back into) the aqueous phase due to its high water solubility (Henry's law constant of
296 $3.1 \times 10^5 \text{ M atm}^{-1}$).⁹² The aqueous phase photochemistry is then competitive with the gas-phase
297 direct photolysis as a sink for pyruvic acid.⁹³ In clouds and fogs, some pyruvic acid undergoes OH
298 oxidation to yield acetic acid, CO₂, and oxalic acid through a glyoxylic acid intermediate.¹⁹
299 Because of the multistep chemistry, conversion of pyruvic to oxalic acid takes hours and occurs
300 over multiple cloud cycles or in a persistent fog. Aqueous dehydrated pyruvic acid is light-
301 absorbing and can undergo direct photolysis or photosensitized reactions resulting in acetoin, lactic
302 and acetic acid, and oligomers through the excited triplet state of the carbonyl oxygen.^{26,28}
303 However, dark reactions in clouds and fogs can also occur. Dicarboxyls similar to pyruvic acid
304 such as glyoxal and methylglyoxal can oligomerize in evaporating droplets.^{29,30,32,35,94} This work
305 shows the potential for pyruvic acid to oligomerize during cloud and fog droplet evaporation.

306 Figure 4 depicts the volatility evolution of aqueous solutions of pyruvic acid. The box in the
307 upper left-hand corner shows volatile and semivolatile carboxylic acids that are highly water
308 soluble, often result from aqueous oxidation, and partition readily into droplets. Processes reducing

the volatility of these compounds can increase the fraction of organic mass that remains in the particle phase after water evaporation. Among these is pyruvic acid, with a vapor pressure of $\sim 10^2$ Pa at 20°C.^{95,96} Aqueous OH-radical initiated oxidation, dark acid-catalyzed accretion reactions and, salt formation of pyruvic acid (not shown) have the potential to reduce the volatility of pyruvic acid. Aqueous OH oxidation of pyruvic acid forms acetic acid, glyoxylic acid, and subsequently oxalic acid, whose vapor pressure is in the semivolatile range ($p^o = 10^{-2}$ to 10^{-4} Pa).^{97,98} The preference of oxalic acid for the particle phase in the atmosphere is likely due to the formation of low volatility oxalate salts or complexes.^{4,12,99} This work suggests that evaporating pyruvic acid solution droplets at aerosol, fog, cloud-relevant concentrations and atmospheric temperatures (10–25°C), in the absence of an inorganic catalyst, leads to formation of acetals and/or cyclic dimers with estimated vapor pressures of 4×10^{-5} Pa¹⁰⁰ and 10–30% volumetric yields. This mechanism could compete with photochemical sinks for pyruvic acid during cloud cycling under dark conditions.

Although the vapor pressure of dimers of pyruvic acid is significantly lower than that of pyruvic acid, they are still considered semivolatile. Dimerization enhances the partitioning of monomers to the condensed phase.³⁶ The formed dimers, especially those with unsaturated double bonds, can participate in additional condensed-phase reactions. For example, the pyruvic acid dimers shown in Figure S5 have been shown to partition to the air-water interface,¹⁰¹ where they may have enhanced reactivity for subsequent reactions.³⁸ The formation of surface active unsaturated dimers from carbonyls such as pyruvic acid during cloud or fog evaporation is one way in which carbon can be transformed in the atmosphere and influence atmospheric chemistry.

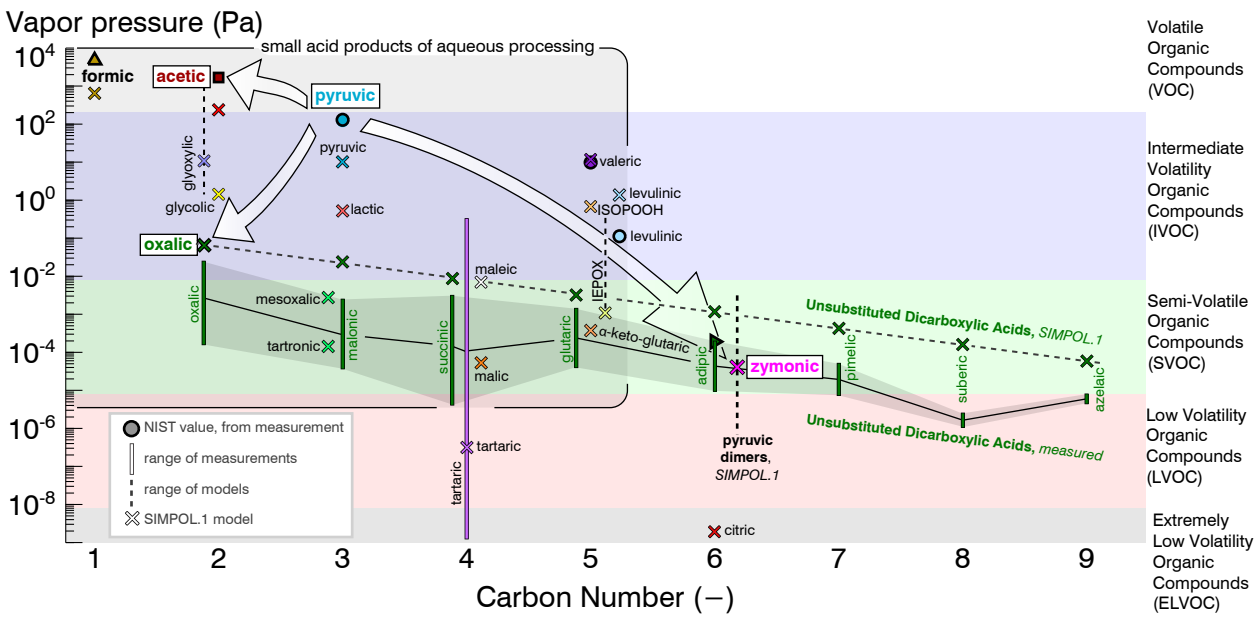


Figure 4. Vapor pressures of pyruvic acid reaction products compared to past organic measurements (20°C),¹⁰² SIMPOL.1¹⁰⁰ -estimated vapor pressures, and volatility ranges defined by Donahue et al.³⁴ Pyruvic dimers include several multifunctional cyclic acids (Figure S3).

Supporting Information. Instrument modifications and schematic; oxidation details; modeling details; reaction mechanisms.

Corresponding Author

*Sarah S. Petters, spetters@unc.edu.

Present Addresses

†now at Institut de Recherches sur la Catalyse et l'Environnement de Lyon (IRCELYON), CNRS, and Université Lyon 1, Villeurbanne, 69626 France.

Funding Sources

This project was funded by the U.S. National Science Foundation Postdoctoral Fellowship under Award #AGS-1624696. REHM was supported by the U.K. Engineering and Physical Sciences Research Council, grant number EP/N025245/1. We thank Sara Duncan for assistance with some of the experiments.

5. References

- (1) Mao, J.; Carlton, A.; Cohen, R. C.; Brune, W. H.; Brown, S. S.; Wolfe, G. M.; Jimenez, J. L.; Pye, H. O. T.; Lee Ng, N.; Xu, L.; et al. Southeast Atmosphere Studies: Learning from Model-Observation Syntheses. *Atmos. Chem. Phys.* **2018**, *18* (4), 2615–2651. doi: 10.5194/acp-18-2615-2018.
- (2) Chan Miller, C.; Jacob, D. J.; Marais, E. A.; Yu, K.; Travis, K. R.; Kim, P. S.; Fisher, J. A.; Zhu, L.; Wolfe, G. M.; Hanisco, T. F.; et al. Glyoxal Yield from Isoprene Oxidation and Relation to Formaldehyde: Chemical Mechanism, Constraints from SENEX Aircraft Observations, and Interpretation of OMI Satellite Data. *Atmos. Chem. Phys.* **2017**, *17* (14), 8725–8738. doi: 10.5194/acp-17-8725-2017.
- (3) Marais, E. A.; Jacob, D. J.; Jimenez, J. L.; Campuzano-Jost, P.; Day, D. A.; Hu, W.; Krechmer, J.; Zhu, L.; Kim, P. S.; Miller, C. C.; et al. Aqueous-Phase Mechanism for Secondary Organic Aerosol Formation from Isoprene: Application to the Southeast United States and Co-Benefit of SO₂ Emission Controls. *Atmos. Chem. Phys.* **2016**, *16* (3), 1603–1618. doi: 10.5194/acp-16-1603-2016.

- (4) Ervens, B.; Turpin, B. J.; Weber, R. J. Secondary Organic Aerosol Formation in Cloud Droplets and Aqueous Particles (AqSOA): A Review of Laboratory, Field and Model Studies. *Atmos. Chem. Phys.* **2011**, *11* (21), 11069–11102. doi: 10.5194/acp-11-11069-2011.
- (5) Blando, J. D.; Turpin, B. J. Secondary Organic Aerosol Formation in Cloud and Fog Droplets: A Literature Evaluation of Plausibility. *Atmos. Environ.* **2000**, *34* (10), 1623–1632. doi: 10.1016/S1352-2310(99)00392-1.
- (6) Budisulistiorini, S. H.; Canagaratna, M. R.; Croteau, P. L.; Marth, W. J.; Baumann, K.; Edgerton, E. S.; Shaw, S. L.; Knipping, E. M.; Worsnop, D. R.; Jayne, J. T.; et al. Real-Time Continuous Characterization of Secondary Organic Aerosol Derived from Isoprene Epoxydiols in Downtown Atlanta, Georgia, Using the Aerodyne Aerosol Chemical Speciation Monitor. *Environ. Sci. Technol.* **2013**, *47* (11), 5686–5694. doi: 10.1021/es400023n.
- (7) McVay, R.; Ervens, B. A Microphysical Parameterization of AqSOA and Sulfate Formation in Clouds. *Geophys. Res. Lett.* **2017**, *44* (14), 7500–7509. doi: 10.1002/2017GL074233.
- (8) Woo, J. L.; McNeill, V. F. SimpleGAMMA v1.0 – a Reduced Model of Secondary Organic Aerosol Formation in the Aqueous Aerosol Phase (AaSOA). *Geosci. Model. Dev.* **2015**, *8* (6), 1821–1829. doi: 10.5194/gmd-8-1821-2015.
- (9) Heald, C. L.; Coe, H.; Jimenez, J. L.; Weber, R. J.; Bahreini, R.; Middlebrook, A. M.; Russell, L. M.; Jolleys, M.; Fu, T.-M.; Allan, J. D.; et al. Exploring the Vertical Profile of Atmospheric Organic Aerosol: Comparing 17 Aircraft Field Campaigns with a Global Model. *Atmos. Chem. Phys.* **2011**, *11* (24), 12673–12696. doi: 10.5194/acp-11-12673-2011.
- (10) Carlton, A. G.; Turpin, B. J.; Altieri, K. E.; Seitzinger, S. P.; Mathur, R.; Roselle, S. J.; Weber, R. J. CMAQ Model Performance Enhanced When In-Cloud Secondary Organic Aerosol Is Included: Comparisons of Organic Carbon Predictions with Measurements. *Environ. Sci. Technol.* **2008**, *42* (23), 8798–8802. doi: 10.1021/es801192n.
- (11) Fu, T.-M.; Jacob, D. J.; Wittrock, F.; Burrows, J. P.; Vrekoussis, M.; Henze, D. K. Global Budgets of Atmospheric Glyoxal and Methylglyoxal, and Implications for Formation of Secondary Organic Aerosols. *J. Geophys. Res. Atmospheres* **2008**, *113*, D15303. doi: 10.1029/2007JD009505.
- (12) Ortiz-Montalvo, D.; Häkkinen, S. A. K.; Schwier, A. N.; Lim, Y. B.; McNeill, V. F.; Turpin, B. J. Ammonium Addition (and Aerosol pH) Has a Dramatic Impact on the Volatility and Yield of Glyoxal Secondary Organic Aerosol. *Environ. Sci. Technol.* **2014**, *48* (1), 255–262. doi: 10.1021/es4035667.
- (13) Carlton, A. G.; Turpin, B. J.; Altieri, K. E.; Seitzinger, S.; Reff, A.; Lim, H.-J.; Ervens, B. Atmospheric Oxalic Acid and SOA Production from Glyoxal: Results of Aqueous

- 397 Photooxidation Experiments. *Atmos. Environ.* **2007**, *41* (35), 7588–7602. doi: 10.1016/
398 j.atmosenv.2007.05.035.
- (14) Tan, Y.; Perri, M. J.; Seitzinger, S. P.; Turpin, B. J. Effects of Precursor Concentration and
Acidic Sulfate in Aqueous Glyoxal–OH Radical Oxidation and Implications for Secondary
Organic Aerosol. *Environ. Sci. Technol.* **2009**, *43* (21), 8105–8112. doi: 10.1021/es901742f.
- (15) Perri, M. J.; Seitzinger, S.; Turpin, B. J. Secondary Organic Aerosol Production from
Aqueous Photooxidation of Glycolaldehyde: Laboratory Experiments. *Atmos. Environ.*
2009, *43* (8), 1487–1497. doi: 10.1016/j.atmosenv.2008.11.037.
- (16) Ortiz-Montalvo, D.; Lim, Y. B.; Perri, M. J.; Seitzinger, S. P.; Turpin, B. J. Volatility and
Yield of Glycolaldehyde SOA Formed through Aqueous Photochemistry and Droplet
Evaporation. *Aerosol Sci. Technol.* **2012**, *46* (9), 1002–1014. doi: 10.1080/
02786826.2012.686676.
- (17) Michaud, V.; El Haddad, I.; Yao Liu; Sellegri, K.; Laj, P.; Villani, P.; Picard, D.; Marchand,
N.; Monod, A. In-Cloud Processes of Methacrolein under Simulated Conditions – Part 3:
Hygroscopic and Volatility Properties of the Formed Secondary Organic Aerosol. *Atmos.*
Chem. Phys. **2009**, *9* (14), 5119–5130. doi: 10.5194/acp-9-5119-2009.
- (18) Tan, Y.; Lim, Y. B.; Altieri, K. E.; Seitzinger, S. P.; Turpin, B. J. Mechanisms Leading to
Oligomers and SOA through Aqueous Photooxidation: Insights from OH Radical Oxidation
of Acetic Acid and Methylglyoxal. *Atmos. Chem. Phys.* **2012**, *12* (2), 801–813. doi:
10.5194/acp-12-801-2012.
- (19) Tan, Y.; Carlton, A. G.; Seitzinger, S. P.; Turpin, B. J. SOA from Methylglyoxal in Clouds
and Wet Aerosols: Measurement and Prediction of Key Products. *Atmos. Environ.* **2010**, *44*
(39), 5218–5226. doi: 10.1016/j.atmosenv.2010.08.045.
- (20) Lim, Y. B.; Turpin, B. J. Laboratory Evidence of Organic Peroxide and Peroxyhemiacetal
Formation in the Aqueous Phase and Implications for Aqueous OH. *Atmos. Chem. Phys.*
2015, *15* (22), 12867–12877. doi: 10.5194/acp-15-12867-2015.
- (21) Ortiz-Montalvo, D.; Schwier, A. N.; Lim, Y. B.; McNeill, V. F.; Turpin, B. J. Volatility of
Methylglyoxal Cloud SOA Formed through OH Radical Oxidation and Droplet
Evaporation. *Atmos. Environ.* **2016**, *130*, 145–152. doi: 10.1016/j.atmosenv.2015.12.013.
- (22) Renard, P.; Reed Harris, A. E.; Rapf, R. J.; Ravier, S.; Demelas, C.; Coulomb, B.; Quivet,
E.; Vaida, V.; Monod, A. Aqueous Phase Oligomerization of Methyl Vinyl Ketone by
Atmospheric Radical Reactions. *J. Phys. Chem. C* **2014**, *118* (50), 29421–29430. doi:
10.1021/jp5065598.
- (23) Yu, L.; Smith, J.; Laskin, A.; George, K. M.; Anastasio, C.; Laskin, J.; Dillner, A. M.;
Zhang, Q. Molecular Transformations of Phenolic SOA during Photochemical Aging in the
Aqueous Phase: Competition among Oligomerization, Functionalization, and

- Fragmentation. *Atmos. Chem. Phys.* **2016**, *16* (7), 4511–4527. doi: 10.5194/acp-16-4511-2016.
- (24) Altieri, K. E.; Carlton, A. G.; Lim, H.-J.; Turpin, B. J.; Seitzinger, S. P. Evidence for Oligomer Formation in Clouds: Reactions of Isoprene Oxidation Products. *Environ. Sci. Technol.* **2006**, *40* (16), 4956–4960. doi: 10.1021/es052170n.
- (25) Carlton, A. G.; Turpin, B. J.; Lim, H.-J.; Altieri, K. E.; Seitzinger, S. Link between Isoprene and Secondary Organic Aerosol (SOA): Pyruvic Acid Oxidation Yields Low Volatility Organic Acids in Clouds. *Geophys. Res. Lett.* **2006**, *33* (6). doi: 10.1029/2005GL025374.
- (26) Griffith, E. C.; Carpenter, B. K.; Shoemaker, R. K.; Vaida, V. Photochemistry of Aqueous Pyruvic Acid. *Proc. Natl. Acad. Sci. USA* **2013**, *110* (29), 11714. doi: 10.1073/pnas.1303206110.
- (27) Bernard, F.; Ciuraru, R.; Boréave, A.; George, C. Photosensitized Formation of Secondary Organic Aerosols above the Air/Water Interface. *Environ. Sci. Technol.* **2016**, *50* (16), 8678–8686. doi: 10.1021/acs.est.6b03520.
- (28) Rapf, R. J.; Perkins, R. J.; Dooley, M. R.; Kroll, J. A.; Carpenter, B. K.; Vaida, V. Environmental Processing of Lipids Driven by Aqueous Photochemistry of α -Keto Acids. *ACS Cent. Sci.* **2018**, *4* (5), 624–630. doi: 10.1021/acscentsci.8b00124.
- (29) Galloway, M. M.; Powelson, M. H.; Sedehi, N.; Wood, S. E.; Millage, K. D.; Kononenko, J. A.; Rynaski, A. D.; De Haan, D. O. Secondary Organic Aerosol Formation during Evaporation of Droplets Containing Atmospheric Aldehydes, Amines, and Ammonium Sulfate. *Environ. Sci. Technol.* **2014**, *48* (24), 14417–14425. doi: 10.1021/es5044479.
- (30) De Haan, D. O.; Corrigan, A. L.; Tolbert, M. A.; Jimenez, J. L.; Wood, S. E.; Turley, J. J. Secondary Organic Aerosol Formation by Self-Reactions of Methylglyoxal and Glyoxal in Evaporating Droplets. *Environ. Sci. Technol.* **2009**, *43* (21), 8184–8190. doi: 10.1021/es902152t.
- (31) Surratt, J. D.; Chan, A. W. H.; Eddingsaas, N. C.; Chan, M.; Loza, C. L.; Kwan, A. J.; Hersey, S. P.; Flagan, R. C.; Wennberg, P. O.; Seinfeld, J. H. Reactive Intermediates Revealed in Secondary Organic Aerosol Formation from Isoprene. *Proc. Natl. Acad. Sci. USA* **2010**, *107* (15), 6640–6645. doi: 10.1073/pnas.0911114107.
- (32) Lee, A. K. Y.; Zhao, R.; Li, R.; Liggio, J.; Li, S.-M.; Abbatt, J. P. D. Formation of Light Absorbing Organo-Nitrogen Species from Evaporation of Droplets Containing Glyoxal and Ammonium Sulfate. *Environ. Sci. Technol.* **2013**, *47* (22), 12819–12826. doi: 10.1021/es402687w.
- (33) Ervens, B. Progress and Problems in Modeling Chemical Processing in Cloud Droplets and Wet Aerosol Particles. In *Multiphase Environmental Chemistry in the Atmosphere*; ACS

- 468 Symposium Series; American Chemical Society, 2018; Vol. 1299, pp 327–345. doi:
469 10.1021/bk-2018-1299.ch016.
- 470 (34) Donahue, N. M.; Kroll, J. H.; Pandis, S. N.; Robinson, A. L. A Two-Dimensional Volatility
471 Basis Set – Part 2: Diagnostics of Organic-Aerosol Evolution. *Atmos. Chem. Phys.* **2012**, *12*
472 (2), 615–634. doi: 10.5194/acp-12-615-2012.
- 473 (35) Loeffler, K. W.; Koehler, C. A.; Paul, N. M.; De Haan, D. O. Oligomer Formation in
474 Evaporating Aqueous Glyoxal and Methyl Glyoxal Solutions. *Environ. Sci. Technol.* **2006**,
475 *40* (20), 6318–6323. doi: 10.1021/es060810w.
- 476 (36) Barsanti, K. C.; Kroll, J. H.; Thornton, J. A. Formation of Low-Volatility Organic
477 Compounds in the Atmosphere: Recent Advancements and Insights. *J. Phys. Chem. Lett.*
478 **2017**, *8* (7), 1503–1511. doi: 10.1021/acs.jpcclett.6b02969.
- 479 (37) Girod, M.; Moyano, E.; Campbell, D. I.; Cooks, R. G. Accelerated Bimolecular Reactions
480 in Microdroplets Studied by Desorption Electrospray Ionization Mass Spectrometry. *Chem.*
481 *Sci.* **2011**, *2* (3), 501–510. doi: 10.1039/C0SC00416B.
- 482 (38) Marsh, B. M.; Iyer, K.; Cooks, R. G. Reaction Acceleration in Electrospray Droplets: Size,
483 Distance, and Surfactant Effects. *J. Am. Soc. Mass Spectrom.* **2019**. doi: 10.1007/s13361-
484 019-02264-w.
- 485 (39) Bain, R. M.; Pulliam, C. J.; Thery, F.; Cooks, R. G. Accelerated Chemical Reactions and
486 Organic Synthesis in Leidenfrost Droplets. *Angew. Chem. Int. Ed.* **2016**, *55* (35), 10478–
487 10482. doi: 10.1002/anie.201605899.
- 488 (40) Badu-Tawiah, A. K.; Campbell, D. I.; Cooks, R. G. Reactions of Microsolvated Organic
489 Compounds at Ambient Surfaces: Droplet Velocity, Charge State, and Solvent Effects. *J.*
490 *Am. Soc. Mass Spectrom.* **2012**, *23* (6), 1077–1084. doi: 10.1007/s13361-012-0365-3.
- 491 (41) Nguyen, T. B.; Lee, P. B.; Updyke, K. M.; Bones, D. L.; Laskin, J.; Laskin, A.; Nizkorodov,
492 S. A. Formation of Nitrogen- and Sulfur-Containing Light-Absorbing Compounds
493 Accelerated by Evaporation of Water from Secondary Organic Aerosols. *J. Geophys. Res.*
494 *Atmos.* **2012**, *117* (D1). doi: 10.1029/2011JD016944.
- 495 (42) Li, Y.; Yan, X.; Cooks, R. G. The Role of the Interface in Thin Film and Droplet Accelerated
496 Reactions Studied by Competitive Substituent Effects. *Angew. Chem. Int. Ed.* **2016**, *55* (10),
497 3433–3437. doi: 10.1002/anie.201511352.
- 498 (43) Zhong, J.; Kumar, M.; Francisco, J. S.; Zeng, X. C. Insight into Chemistry on Cloud/Aerosol
499 Water Surfaces. *Acc. Chem. Res.* **2018**, *51* (5), 1229–1237. doi: 10.1021/
500 acs.accounts.8b00051.

Manuscript for submission to *ACS Earth and Space Chemistry*

- (44) Eugene, A. J.; Pillar, E. A.; Colussi, A. J.; Guzman, M. I. Enhanced Acidity of Acetic and Pyruvic Acids on the Surface of Water. *Langmuir* **2018**, *34* (31), 9307–9313. doi: 10.1021/acs.langmuir.8b01606.
- (45) Narayan, S.; Muldoon, J.; Finn, M. G.; Fokin, V. V.; Kolb, H. C.; Sharpless, K. B. “On Water”: Unique Reactivity of Organic Compounds in Aqueous Suspension. *Angew. Chem. Int. Ed.* **2005**, *44* (21), 3275–3279. doi: 10.1002/anie.200462883.
- (46) Donaldson, D. J.; Vaida, V. The Influence of Organic Films at the Air–Aqueous Boundary on Atmospheric Processes. *Chem. Rev.* **2006**, *106* (4), 1445–1461. doi: 10.1021/cr040367c.
- (47) Nishino, N.; Hollingsworth, S. A.; Stern, A. C.; Roeselová, M.; Tobias, D. J.; Finlayson-Pitts, B. J. Interactions of Gaseous HNO₃ and Water with Individual and Mixed Alkyl Self-Assembled Monolayers at Room Temperature. *Phys. Chem. Chem. Phys.* **2014**, *16* (6), 2358–2367. doi: 10.1039/C3CP54118E.
- (48) Wingen, L. M.; Moskun, A. C.; Johnson, S. N.; Thomas, J. L.; Roeselová, M.; Tobias, D. J.; Kleinman, M. T.; Finlayson-Pitts, B. J. Enhanced Surface Photochemistry in Chloride–Nitrate Ion Mixtures. *Phys. Chem. Chem. Phys.* **2008**, *10* (37), 5668–5677. doi: 10.1039/B806613B.
- (49) Stefan, M. I.; Bolton, J. R. Reinvestigation of the Acetone Degradation Mechanism in Dilute Aqueous Solution by the UV/H₂O₂ Process. *Environ. Sci. Technol.* **1999**, *33* (6), 870–873. doi: 10.1021/es9808548.
- (50) Kawamura, K.; Tachibana, E.; Okuzawa, K.; Aggarwal, S. G.; Kanaya, Y.; Wang, Z. F. High Abundances of Water-Soluble Dicarboxylic Acids, Ketocarboxylic Acids and α -Dicarbonyls in the Mountaintop Aerosols over the North China Plain during Wheat Burning Season. *Atmos. Chem. Phys.* **2013**, *13* (16), 8285–8302. doi: 10.5194/acp-13-8285-2013.
- (51) Talbot, R. W.; Andreae, M. O.; Berresheim, H.; Jacob, D. J.; Beecher, K. M. Sources and Sinks of Formic, Acetic, and Pyruvic Acids over Central Amazonia: 2. Wet Season. *J. Geophys. Res. Atmos.* **1990**, *95*, 16799–16811. doi: 10.1029/JD095iD10p16799.
- (52) Praplan, A. P.; Hegyi-Gaeggeler, K.; Barmet, P.; Pfaffenberger, L.; Dommen, J.; Baltensperger, U. Online Measurements of Water-Soluble Organic Acids in the Gas and Aerosol Phase from the Photooxidation of 1,3,5-Trimethylbenzene. *Atmos. Chem. Phys.* **2014**, *14* (16), 8665–8677. doi: 10.5194/acp-14-8665-2014.
- (53) Mattila, J. M.; Brophy, P.; Kirkland, J.; Hall, S.; Ullmann, K.; Fischer, E. V.; Brown, S.; McDuffie, E.; Tevlin, A.; Farmer, D. K. Tropospheric Sources and Sinks of Gas-Phase Acids in the Colorado Front Range. *Atmos. Chem. Phys.* **2018**, *18* (16), 12315–12327. doi: 10.5194/acp-18-12315-2018.

- (54) Andino, J. M.; Smith, J. N.; Flagan, R. C.; Goddard, W. A.; Seinfeld, J. H. Mechanism of Atmospheric Photooxidation of Aromatics: A Theoretical Study. *J. Phys. Chem.* **1996**, *100* (26), 10967–10980. doi: 10.1021/jp952935l.
- (55) Veres, P.; Roberts, J. M.; Burling, I. R.; Warneke, C.; de Gouw, J.; Yokelson, R. J. Measurements of Gas-Phase Inorganic and Organic Acids from Biomass Fires by Negative-Ion Proton-Transfer Chemical-Ionization Mass Spectrometry. *J. Geophys. Res. Atmos.* **2010**, *115* (D23). doi: 10.1029/2010JD014033.
- (56) Reed Harris, A. E.; Pajunoja, A.; Cazaunau, M.; Gratien, A.; Pangui, E.; Monod, A.; Griffith, E. C.; Virtanen, A.; Doussin, J.-F.; Vaida, V. Multiphase Photochemistry of Pyruvic Acid under Atmospheric Conditions. *J. Phys. Chem. A* **2017**, *121* (18), 3327–3339. doi: 10.1021/acs.jpca.7b01107.
- (57) Andreae, M. O.; Talbot, R. W.; Li, S.-M. Atmospheric Measurements of Pyruvic and Formic Acid. *J. Geophys. Res. Atmos.* **1987**, *92*, 6635–6641. doi: 10.1029/JD092iD06p06635.
- (58) Guzmán, M. I.; Colussi, A. J.; Hoffmann, M. R. Photoinduced Oligomerization of Aqueous Pyruvic Acid. *J. Phys. Chem. A* **2006**, *110* (10), 3619–3626. doi: 10.1021/jp056097z.
- (59) Schaefer, T.; Schindelka, J.; Hoffmann, D.; Herrmann, H. Laboratory Kinetic and Mechanistic Studies on the OH-Initiated Oxidation of Acetone in Aqueous Solution. *J. Phys. Chem. A* **2012**, *116* (24), 6317–6326. doi: 10.1021/jp2120753.
- (60) Healy, R. M.; Wenger, J. C.; Metzger, A.; Duplissy, J.; Kalberer, M.; Dommen, J. Gas/Particle Partitioning of Carbonyls in the Photooxidation of Isoprene and 1,3,5-Trimethylbenzene. *Atmos. Chem. Phys.* **2008**, *8* (12), 3215–3230. doi: 10.5194/acp-8-3215-2008.
- (61) Berglund, R. N.; Liu, B. Y. H. Generation of Monodisperse Aerosol Standards. *Environ. Sci. Technol.* **1973**, *7* (2), 147–153. doi: 10.1021/es60074a001.
- (62) Werner, F.; Ditas, F.; Siebert, H.; Simmel, M.; Wehner, B.; Pilewskie, P.; Schmeissner, T.; Shaw, R. A.; Hartmann, S.; Wex, H.; et al. Twomey Effect Observed from Collocated Microphysical and Remote Sensing Measurements over Shallow Cumulus. *J. Geophys. Res. Atmos.* **2014**, *119* (3), 1534–1545. doi: 10.1002/2013JD020131.
- (63) Barr, E. B.; Carpenter, R. L.; Newton, G. J. Improved Liquid Feed System for the Berglund-Liu Vibrating Orifice Monodisperse Aerosol Generator. *Environ. Sci. Technol.* **1984**, *18* (9), 721–723. doi: 10.1021/es00127a016.
- (64) Devarakonda, V.; Ray, A. K.; Kaiser, T.; Schweiger, G. Vibrating Orifice Droplet Generator for Studying Fast Processes Associated with Microdroplets. *Aerosol Sci. Technol.* **1998**, *28* (6), 531–547. doi: 10.1080/02786829808965544.

Manuscript for submission to *ACS Earth and Space Chemistry*

- (65) Mavrogiannis, N.; Ibo, M.; Fu, X.; Crivellari, F.; Gagnon, Z. Microfluidics Made Easy: A Robust Low-Cost Constant Pressure Flow Controller for Engineers and Cell Biologists. *Biomicrofluidics* **2016**, *10* (3), 034107. doi: 10.1063/1.4950753.
- (66) Petters, M. D.; Kreidenweis, S. M.; Prenni, A. J.; Sullivan, R. C.; Carrico, C. M.; Koehler, K. A.; Ziemann, P. J. Role of Molecular Size in Cloud Droplet Activation. *Geophys. Res. Lett.* **2009**, *36* (22), L22801. doi: 10.1029/2009GL040131.
- (67) Petters, S. S.; Pagonis, D.; Claflin, M. S.; Levin, E. J. T.; Petters, M. D.; Ziemann, P. J.; Kreidenweis, S. M. Hygroscopicity of Organic Compounds as a Function of Carbon Chain Length and Carboxyl, Hydroperoxy, and Carbonyl Functional Groups. *J. Phys. Chem. A* **2017**, *121* (27), 5164–5174. doi: 10.1021/acs.jpca.7b04114.
- (68) Davies, J. F.; Haddrell, A. E.; Reid, J. P. Time-Resolved Measurements of the Evaporation of Volatile Components from Single Aerosol Droplets. *Aerosol Sci. Technol.* **2012**, *46* (6), 666–677. doi: 10.1080/02786826.2011.652750.
- (69) Rovelli, G.; Miles, R. E. H.; Reid, J. P.; Clegg, S. L. Accurate Measurements of Aerosol Hygroscopic Growth over a Wide Range in Relative Humidity. *J. Phys. Chem. A* **2016**, *120* (25), 4376–4388. doi: 10.1021/acs.jpca.6b04194.
- (70) Su, Y.-Y.; Marsh, A.; Haddrell, A. E.; Li, Z.-M.; Reid, J. P. Evaporation Kinetics of Polyol Droplets: Determination of Evaporation Coefficients and Diffusion Constants. *J. Geophys. Res. Atmos.* **2017**, *122* (22), 12,317–12,334. doi: 10.1002/2017JD027111.
- (71) Dawson, K. W.; Petters, M. D.; Meskhidze, N.; Petters, S. S.; Kreidenweis, S. M. Hygroscopic Growth and Cloud Droplet Activation of Xanthan Gum as a Proxy for Marine Hydrogels. *J. Geophys. Res. Atmos.* **2016**, *121* (19), 11803–11818. doi: 10.1002/2016JD025143.
- (72) Tomaz, S.; Cui, T.; Chen, Y.; Sexton, K. G.; Roberts, J. M.; Warneke, C.; Yokelson, R. J.; Surratt, J. D.; Turpin, B. J. Photochemical Cloud Processing of Primary Wildfire Emissions as a Potential Source of Secondary Organic Aerosol. *Environ. Sci. Technol.* **2018**, *52* (19), 11027–11037. doi: 10.1021/acs.est.8b03293.
- (73) van Pinxteren, D.; Fomba, K. W.; Mertes, S.; Müller, K.; Spindler, G.; Schneider, J.; Lee, T.; Collett, J. L.; Herrmann, H. Cloud Water Composition during HCCT-2010: Scavenging Efficiencies, Solute Concentrations, and Droplet Size Dependence of Inorganic Ions and Dissolved Organic Carbon. *Atmospheric Chem. Phys.* **2016**, *16* (5), 3185–3205. doi: 10.5194/acp-16-3185-2016.
- (74) Deguillaume, L.; Charbouillot, T.; Joly, M.; Vaïtilingom, M.; Parazols, M.; Marinoni, A.; Amato, P.; Delort, A.-M.; Vinatier, V.; Flossmann, A.; et al. Classification of Clouds Sampled at the Puy de Dôme (France) Based on 10 Yr of Monitoring of Their Physicochemical Properties. *Atmos. Chem. Phys.* **2014**, *14* (3), 1485–1506. doi: 10.5194/acp-14-1485-2014.

- (75) Lim, Y. B.; Tan, Y.; Turpin, B. J. Chemical Insights, Explicit Chemistry, and Yields of Secondary Organic Aerosol from OH Radical Oxidation of Methylglyoxal and Glyoxal in the Aqueous Phase. *Atmos. Chem. Phys.* **2013**, *13* (17), 8651–8667. doi: 10.5194/acp-13-8651-2013.
- (76) Herrmann, H.; Hoffmann, D.; Schaefer, T.; Brüner, P.; Tilgner, A. Tropospheric Aqueous-Phase Free-Radical Chemistry: Radical Sources, Spectra, Reaction Kinetics and Prediction Tools. *Chem. Phys. Phys. Chem.* **2010**, *11* (18), 3796–3822. doi: 10.1002/cphc.201000533.
- (77) Arakaki, T.; Anastasio, C.; Kuroki, Y.; Nakajima, H.; Okada, K.; Kotani, Y.; Handa, D.; Azechi, S.; Kimura, T.; Tsuchioka, A.; et al. A General Scavenging Rate Constant for Reaction of Hydroxyl Radical with Organic Carbon in Atmospheric Waters. *Environ. Sci. Technol.* **2013**, *47* (15), 8196–8203. doi: 10.1021/es401927b.
- (78) Ahn, K.-H.; Liu, B. Y. H. Particle Activation and Droplet Growth Processes in Condensation Nucleus Counter—I. Theoretical Background. *J. Aerosol Sci.* **1990**, *21* (2), 249–261. doi: 10.1016/0021-8502(90)90008-L.
- (79) Bilde, M.; Svenningsson, B.; Mønster, J.; Rosenørn, T. Even–Odd Alternation of Evaporation Rates and Vapor Pressures of C3–C9 Dicarboxylic Acid Aerosols. *Environ. Sci. Technol.* **2003**, *37* (7), 1371–1378. doi: 10.1021/es0201810.
- (80) Hinds, W. C. *Aerosol Technology: Properties, Behavior, and Measurement of Airborne Particles*, 2nd ed.; John Wiley and Sons: New York, 1999.
- (81) Davis, E. J.; Ray, A. K. Submicron Droplet Evaporation in the Continuum and Non-Continuum Regimes. *J. Aerosol Sci.* **1978**, *9* (5), 411–422. doi: 10.1016/0021-8502(78)90003-4.
- (82) Hirschfelder, J. O.; Curtiss, C. F.; Bird, R. B. *Molecular Theory of Gases and Liquids*; Wiley, 1967.
- (83) Lim, H.-J.; Carlton, A. G.; Turpin, B. J. Isoprene Forms Secondary Organic Aerosol Through Cloud Processing: Model Simulations. *Environ. Sci. Technol.* **2005**, *39* (12), 4441–4446. doi: 10.1021/es048039h.
- (84) Suda, S. R.; Petters, M. D. Accurate Determination of Aerosol Activity Coefficients at Relative Humidities up to 99% Using the Hygroscopicity Tandem Differential Mobility Analyzer Technique. *Aerosol Sci. Technol.* **2013**, *47* (9), 991–1000. doi: 10.1080/02786826.2013.807906.
- (85) Suda, S. R.; Petters, M. D.; Matsunaga, A.; Sullivan, R. C.; Ziemann, P. J.; Kreidenweis, S. M. Hygroscopicity Frequency Distributions of Secondary Organic Aerosols. *J. Geophys. Res. Atmos.* **2012**, *117*, D04207. doi: 10.1029/2011JD016823.

- (86) Pocker, Y.; Meany, J. E.; Nist, B. J.; Zadorojny, C. Reversible Hydration of Pyruvic Acid. I. Equilibrium Studies. *J. Phys. Chem.* **1969**, *73* (9), 2879–2882. doi: 10.1021/j100843a015.
- (87) Liggio, J.; Li, S.-M.; McLaren, R. Heterogeneous Reactions of Glyoxal on Particulate Matter: Identification of Acetals and Sulfate Esters. *Environ. Sci. Technol.* **2005**, *39* (6), 1532–1541. doi: 10.1021/es048375y.
- (88) Rapf, R. J.; Dooley, M. R.; Kappes, K.; Perkins, R. J.; Vaida, V. PH Dependence of the Aqueous Photochemistry of α -Keto Acids. *J. Phys. Chem. A* **2017**, *121* (44), 8368–8379. doi: 10.1021/acs.jpca.7b08192.
- (89) Perkins, R. J.; Shoemaker, R. K.; Carpenter, B. K.; Vaida, V. Chemical Equilibria and Kinetics in Aqueous Solutions of Zymonic Acid. *J. Phys. Chem. A* **2016**, *120* (51), 10096–10107. doi: 10.1021/acs.jpca.6b10526.
- (90) Otto, T.; Stieger, B.; Mettke, P.; Herrmann, H. Tropospheric Aqueous-Phase Oxidation of Isoprene-Derived Dihydroxycarbonyl Compounds. *J. Phys. Chem. A* **2017**, *121* (34), 6460–6470. doi: 10.1021/acs.jpca.7b05879.
- (91) Mellouki, A.; Mu, Y. On the Atmospheric Degradation of Pyruvic Acid in the Gas Phase. *Atmos. Photochem.* **2003**, *157* (2), 295–300. doi: 10.1016/S1010-6030(03)00070-4.
- (92) Sander, R. Compilation of Henry's Law Constants (Version 4.0) for Water as Solvent. *Atmos. Chem. Phys.* **2015**, *15* (8), 4399–4981. doi: 10.5194/acp-15-4399-2015.
- (93) Epstein, S. A.; Nizkorodov, S. A. A Comparison of the Chemical Sinks of Atmospheric Organics in the Gas and Aqueous Phase. *Atmos. Chem. Phys.* **2012**, *12* (17), 8205–8222. doi: 10.5194/acp-12-8205-2012.
- (94) Herrmann, H.; Schaefer, T.; Tilgner, A.; Styler, S. A.; Weller, C.; Teich, M.; Otto, T. Tropospheric Aqueous-Phase Chemistry: Kinetics, Mechanisms, and Its Coupling to a Changing Gas Phase. *Chem. Rev.* **2015**, *115* (10), 4259–4334. doi: 10.1021/cr500447k.
- (95) Stull, D. R. Inorganic Compounds. *Ind. Eng. Chem.* **1947**, *39* (4), 540–550. doi: 10.1021/ie50448a023.
- (96) Emel'yanenko, V. N.; Turovtsev, V. V.; Fedina, Y. A. Thermodynamic Properties of Pyruvic Acid and Its Methyl Ester. *Thermochim. Acta* **2018**, *665*, 70–75. doi: 10.1016/j.tca.2018.05.009.
- (97) Soonsin, V.; Zardini, A. A.; Marcolli, C.; Zuend, A.; Krieger, U. K. The Vapor Pressures and Activities of Dicarboxylic Acids Reconsidered: The Impact of the Physical State of the Aerosol. *Atmos. Chem. Phys.* **2010**, *10* (23), 11753–11767. doi: 10.5194/acp-10-11753-2010.

Manuscript for submission to *ACS Earth and Space Chemistry*

- (98) Booth, A. M.; Barley, M. H.; Topping, D. O.; McFiggans, G.; Garforth, A.; Percival, C. J. Solid State and Sub-Cooled Liquid Vapour Pressures of Substituted Dicarboxylic Acids Using Knudsen Effusion Mass Spectrometry (KEMS) and Differential Scanning Calorimetry. *Atmos. Chem. Phys.* **2010**, *10* (10), 4879–4892. doi: 10.5194/acp-10-4879-2010.
- (99) Paciga, A. L.; Riipinen, I.; Pandis, S. N. Effect of Ammonia on the Volatility of Organic Diacids. *Environ. Sci. Technol.* **2014**, *48* (23), 13769–13775. doi: 10.1021/es5037805.
- (100) Pankow, J. F.; Asher, W. E. SIMPOL.1: A Simple Group Contribution Method for Predicting Vapor Pressures and Enthalpies of Vaporization of Multifunctional Organic Compounds. *Atmos. Chem. Phys.* **2008**, *8* (10), 2773–2796. doi: 10.5194/acp-8-2773-2008.
- (101) Gordon, B. P.; Moore, F. G.; Scatena, L.; Richmond, G. L. On the Rise: Experimental and Computational VSFS Studies of Pyruvic Acid and Its Surface Active Oligomer Species at the Air-Water Interface. *J. Phys. Chem. A* **2019**. doi: 10.1021/acs.jpca.9b08854.
- (102) Bilde, M.; Barsanti, K.; Booth, M.; Cappa, C. D.; Donahue, N. M.; Emanuelsson, E. U.; McFiggans, G.; Krieger, U. K.; Marcolli, C.; Topping, D.; et al. Saturation Vapor Pressures and Transition Enthalpies of Low-Volatility Organic Molecules of Atmospheric Relevance: From Dicarboxylic Acids to Complex Mixtures. *Chem. Rev.* **2015**, *115* (10), 4115–4156. doi: 10.1021/cr5005502.

Pyruvic Acid *in* Evaporating Droplets

Page 29 of 33 ACS Earth and Space Chemistry

